International Journal of Industrial Engineering Computations 15 (2024) 457–472

Contents lists available at GrowingScience

International Journal of Industrial Engineering Computations

homepage: www.GrowingScience.com/ijiec

Truck-drone joint path planning for post-disaster emergency material deployment considering fairness

Wei Hong[a,b,c]*, Shuaichen Liu[a], Shuling Xu[a] and Xujin Pu[a,b,c]

[a]*School of Business, Jiangnan University, Wuxi, 214122, China*
[b]*Food Safety Research Base of Jiangsu Province, Jiangnan University, Wuxi, 214122, China*
[c]*Institute for Food Safety Risk Management, Jiangnan University, Wuxi, 214122, China*

C H R O N I C L E

Article history:
Received October 20 2023
Received in Revised Format December 18 2023
Accepted January 10 2024
Available online January 10 2024

Keywords:
Fairness
Truck
Drone
Path Planning
Two-Stage Heuristic Algorithm

A B S T R A C T

As the expert gear of the emergency rescue system, drones are frequently utilized to distribute supplies following a calamity. The cost and effectiveness of rescue efforts as well as equitable distribution should be taken into account when allocating emergency supplies to disaster-affected areas. This work explores the emergency material allocation problem for truck-drone joint transportation with dynamic energy restrictions based on taking the fairness of emergency material allocation into consideration. In order to guarantee the equitable distribution of materials, the psychological stress experienced by the victims at each catastrophe site is measured using the relative deprivation cost. An adaptive large-scale neighborhood search method serves as the foundation for the creation of a two-stage heuristic algorithm, which reduces the overall cost of the system. The integer programming model MIP is built for this purpose. The research findings can serve as a useful guide for developing a just and effective emergency drone rescue system, and the testing results demonstrate the viability and effectiveness of the two-stage heuristic algorithm.

1. Introduction

Given the unique circumstances, such as the post-disaster traffic impediment or the isolation of the disaster-hit site, the truck transport alone cannot effectively complete the material distribution task at the demand point following an earthquake, flood, or any other natural disaster or public health incident. As a result, a post-disaster emergency logistics system based on truck travel has formed, supplemented by air transport. Drones, which are specialized equipment used in emergency rescue operations, depend on ground control systems to plan routes that would enable them to fly steadily and precisely inside a limited area, allowing them to deliver emergency supplies to victims at the catastrophe site (Poikonen & Campbell, 2021). The distribution of emergency supplies in disaster areas is a vital component of humanitarian relief efforts. While supplies are being distributed, victims of the psychological trauma brought on by the incident cannot be overlooked (Holguín-Veras et al., 2013). Ethical and efficient decision-making regarding the distribution of supplies can help lessen the suffering of disaster victims (Gutjahr & Nolz, 2016). Based on this, this paper will investigate how to set up a truck-drone joint transport emergency material deployment program that works well in the post-disaster emergency logistics scenario. The goal is to ensure that victims of the disaster receive emergency supplies while also having their psychological trauma fairly mitigated.

Drones have started to become a vital component of the commercial logistics system in recent years. "Amazon Prime Air," the company's first commercial drone delivery initiative, was unveiled by Amazon in 2013 (D'Andrea, 2014). Businesses have introduced drone delivery business strategies in the ten years that have passed. The American professor Wohlsen (2014) notes that parcel transportation could become more affordable and faster than ever before if vehicles and drones are paired for distribution. Additionally, using a truck and drone combination to distribute non-contact materials in the wake of natural

* Corresponding author
E-mail hongwei@jiangnan.edu.cn (W. Hong)
ISSN 1923-2934 (Online) - ISSN 1923-2926 (Print)
2024 Growing Science Ltd.
doi: 10.5267/j.ijiec.2024.1.002

disasters or public health emergencies has proven to be a successful strategy for helping the government and nonprofits meet package delivery demands while addressing the difficulties posed by disasters. Drones can provide non-contact, differential distribution in this emergency by replacing rescuers; this has surely expedited the development of drone distribution inside the emergency logistics system (Chowdhury et al.,2021). According to the information that is currently available, trucks and drones work well together, and each has advantages of its own. The truck has moderate speed, a big weight, muscular endurance, and so on. In contrast, the drone has high speed, a tiny load, and poor endurance. Since they are not constrained by traffic congestion or road networks, drones typically travel at a higher speed than trucks. Nevertheless, the drones can only transport one or more goods at a time due to their very small payload capacities. The fact that they depend on comparatively tiny battery-powered aircraft, which have a shorter range than fuel- or high-capacity battery-powered vehicles, is more significant. Given the truck and drone's complementary qualities, integrating drones into the "last mile" distribution network is probably going to result in more synergy. When both are used together, operating time can be greatly shortened, and distribution efficiency is raised.

Early on in natural disasters, there has been a marked increase in the need for emergency supplies at all disaster-affected locations. Victims' psychological trauma also increases, albeit to varying degrees, during the process of distributing emergency supplies by drone. In a systematic study of the theory of relative deprivation in humanitarian relief, José Holguín-Veras et al. (2012) noted that when deciding how to deploy emergency response materials, it is important to consider the victims' relative sense of deprivation at each disaster site. They also used a tool called the “Deprivation Cost” to calculate the psychological trauma that victims at each disaster site would suffer because of not receiving emergency response materials in a timely manner. One important factor in reducing the pain of catastrophe victims is the equitable distribution of emergency supplies. Further investigation by Gutjahr and Fischer (2018) shown that injustice frequently occurs because of the relentless pursuit of “minimization of the cost of deprivation” in disaster-affected areas. Zhu et al. (2019) propose “Relative Deprivation Cost” as a means of measuring the psychological trauma that victims of disasters experience at different disaster-affected points because of not receiving emergency materials in a timely manner. They argue that the principle of fairness in humanitarian relief should be reflected in the decision-making process by lowering the total value of the relative deprivation cost in the disaster-affected areas. In conclusion, the current state of truck-drone joint transportation makes it relatively uncommon to take into account the fair allocation of emergency supplies path planning problem. For this reason, this paper studied the issue of fair allocation of emergency supplies in the truck-drone joint transportation by stages in conjunction with the drone energy consumption estimation model. The present study differs in that it: 1) examines the use of truck transport drones and drones carrying multiple emergency supplies to achieve multiple distribution disaster sites; 2) constructs a mixed integer programming model (MIP) taking into account the constraints of truck capacity, drone energy consumption, and load; and 3) designs a two-stage heuristic algorithm, TD-TSH, based on large-scale neighborhood search algorithm to solve the combinatorial optimization problem.

2. Related Works

This study mainly involves the following two different dimensions that is, the truck-drone combined transportation optimization and the decision-making objective of post-disaster emergency logistics path optimization.

2.1 Truck-Drone Combined Transportation Optimization

It is necessary to consider the load capacity constraints of drones when trucks and drones jointly undertake the task of emergency material distribution. Murray et al. (2015) studied the cooperative distribution of single drone and single truck and constructed the FSTSP (Flying Sidekick TSP) model and PDSTSP (Parallel Drum Scheduling TSP) model based on the TSP (Traveling Salesman Problem) model. The load level of the drone plays an essential role in both models. Agatz et al. (2018) proposed the TSPD (Traveling Salesman Problem with Drones) model based on FSTSP; a fundamental assumption is that drones can be released or recovered by trucks at the exact location. Wang and Sheu (2019) extended the model based on the research of Murry and constructed the path planning model of multi-drone and multi-truck cooperative distribution as VRPD (Vehicle Routing Problem with Drones) model. Given the specific number of drones and the speed of drones, the vital influence of drone load capacity on flight path decision-making was studied.

As drones are usually powered by batteries, the endurance limit of drones is often considered when they undertake the task of emergency material distribution. Dorling et al. (2016) put forward the drone energy consumption estimation model through the experimental method. The dynamic load data of drones and their lifetime are linked together. The impact of the weight of the drone battery, the weight of loaded goods, and the number of drones on the total distribution cost and the total distribution time are studied. Jeong et al. (2019) proposed the FSTSP-ECNZ (FSTSP that implements energy summation and no-fly zone) model based on it. The influence of no-fly zone on drone distribution path is further studied while considering the influence of drone load weight on drone energy consumption.

For the cooperative problem of single-truck and multi-drones, the relevant research can be traced back to the truck-drone path problem with relay location introduced by Mourelo Ferrandez et al. (2016). The dynamic truck-drone distribution network was transformed into a static relay location problem without fixed cost, and the problem was solved by K-means clustering and genetic algorithm. One fundamental assumption is that trucks wait in place until the fleet returns to the following relay site after releasing the drone fleet at one relay site. Under the same assumptions, Chang and Lee (2018) proposed a non-linear programming model. Relay location is selected based on K-Means clustering, and it is verified that adding shift weight is effective in generating the truck path with drones. Similarly, Moshref-Javadi et al. (2020) introduced the Multi-trip Traveling Repairman Problem with Drones (MTRPD) to minimize the customer waiting time, Vu et al. (2022) proposed the two-echelon routing problem with trucks and drones (2ER-TD) to minimize the delivery operation time of trucks and drones. Based on the above research, this paper studies the coordination problem of single-truck and multi-drone, adding the dynamic energy consumption constraints of drones and designing more realistic conditions of the truck-drone joint transport of emergency supplies allocation problem.

2.2 Decision-making Objective of Post-disaster Emergency Logistics Path Optimization

Economic cost reduction or distribution distance cost reduction are typically the main goals of the conventional decision-making processes employed in commercial logistics path optimization. However, path decision-making frequently needs to take rescue efficiency, rescue efficiency, and whether the rescue is fair into consideration. This is because the relevant literature on the disaster emergency logistics rescue path decision is based on the humanitarian aspects of disaster relief (Huang, 2012). Rescue efficiency is a conventional goal of decision-making, mostly determined by the financial implications of the rescue. For instance, the effectiveness of rescue operations is frequently assessed using the cost of resource allocation and the cost of road transport (Rodríguez-Espíndola et al., 2018; Moreno et al., 2020), which is quite like the general commercial logistics industry's performance evaluation index.

Rescue efficiency, which primarily includes the post-disaster rescue response time, the viability of the rescue plan, and the decrease in casualties in the disaster area, is a crucial criterion to assess the effectiveness or impact of path optimization. To assess the benefits of the medical vehicle relief approach, Xiang and Zhuang (2016) suggested lowering both the overall waiting time and the anticipated death rate of the catastrophe victims. As a shared goal of the rescue decision, Sun et al. (2021) focused on decreasing the severity of minor and severe post-disaster injuries and minimizing the total system expenses of the rescue operation. The “cost of deprivation” idea was first presented by Pérez-Rodríguez and Holguín-Veras (2016) in order to measure the psychological and physical harm that people experience as a result of a lack of resources or assistance. Social cost minimization—that is, the cost of logistics, the cost of deprivation, and other costs—is taken into consideration while making decisions in the emergency that follows a tragedy. This approach may be more effective for path optimization. Based on the notion of deprivation cost, Wang et al. (2017) proposed the “deprivation level” and used a digital evaluation scale to estimate the function of the deprivation level. A typical S-type logistic growth function is suggested as an expression for the deprivation level based on the examination of the data provided by the interviewees, which can be integrated into the humanitarian logistic optimization model to consider human suffering better.

In order to maximize the post-disaster emergency logistics path, it is becoming increasingly important to prioritize equitable rescue. In order to ensure that catastrophe victims receive equal treatment with other individuals, the evaluation of the fairness of rescue decision-making should center on whether emergency resources can be used or allocated in a balanced way throughout the rescue operations (Yu et al., 2018, 2019). The current study measures fairness from several aspects using the minimum and maximum fair value, numerical proportional fairness, absolute deprivation, Gini index, and other various quantitative methodologies (Nair et al., 2018; McCoy & Lee, 2014). According to Balcik and Beamon (2008), one of the most important decision objectives for catastrophe emergency path optimization is to minimize unmet demand. Najafi et al. (2013) proposed that because the material satisfaction rate is easy to quantify, it can also be used to measure the fair. Kilic et al. (2014) measured the fairness of treatment standards by reflecting the degree of health inequalities between various service objects in the priority of emergency path options. In conclusion, the pertinent literature on post-disaster emergency logistics path optimization frequently ignores the severity of the victims' poverty, their suffering, and their negative emotions in favor of quantitative numerical indicators or economic cost as a means of gauging fairness. A key indicator of justice is the psychological stress victims experience as they wait for assistance. At the same time, studies have shown that minimizing the cost of deprivation alone will lead to great inequality (Gutjahr & Fischer, 2018). These studies provide a new perspective that considers the extent of trauma experienced by victims and further measures the relationship between efficiency, effectiveness, and fairness.

3. Problem Description and Mathematical model

Considering the truck capacity, drone load, endurance, and the fairness of the emergency material allocation scheme, this study uses the single truck-multi drone combined transport mode; the specific distribution process is shown in Fig. 1. The truck leaves the distribution center, traverses all stops, and eventually returns to the distribution center. When the truck reaches a parking point, the drones are released to carry out the emergency material distribution work to the disaster-affected sites around. After the drone completes the distribution task, the emergency material is recovered into the truck, the battery is changed, and the truck moves to the next parking point to continue the emergency material distribution work until the distribution work of all the disaster-affected sites is completed.

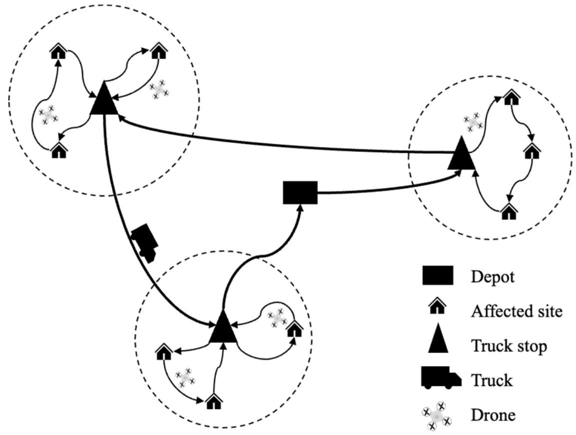

Fig. 1. Illustration of the Combined Transportation Process

3.1 Parameter Definition and Model Assumptions

Note that the set of all disaster sites in the affected area is $N = \{1, 2, \cdots, n\}$, the two-dimensional coordinate of the disaster sites is (A_z, B_z), $\forall z \in N$, and the number of disaster sites is n. The cluster centers, the truck stops, are grouped into $J = \{n + 1, n + 2, \cdots, n + m\}$, and the number of the cluster centers is m. The disaster sites and cluster centers are grouped as $V = N \cup J = \{1, 2, \cdots, n + 1, n + 2, \cdots, n + m\}$, with a total of $n + m$ nodes. The distribution center is denoted as O, then the distribution center and the cluster centers are denoted as set $J' = J \cup \{O\}$. Note that emergency materials collection is $D = \{1, 2, \cdots, s\}$, and the unit weight of emergency material d is $g_d, \forall d \epsilon D$. The demand for emergency material d at disaster site i is $Q_{id}, \forall i \in N, d \in D$. The distribution of emergency material d to disaster site i is $q_{id}, q_{id} \leq Q_{id}, \forall i \in N, d \in D$. The total emergency material assigned to disaster site i is $w_i, w_i = \sum_{d \in D} g_d q_{id}, \forall i \in N$. The unit path cost of the truck is C_{truck}. The unit path cost of the drone is C_{drone}, and the maximum safe load of the drone is W. The launch cost incurred after one drone is put into service is L, and the reception cost after one drone is put into service is R. The battery capacity of the drone is E, and the battery energy consumption parameter is η. Set a maximum positive number to M. The decision variables are as follows:
Decision variables (a_z, b_z), $\forall z \in J$;

Decision variables

$$x_{ijm} = \begin{cases} 1, the\ drone\ takes\ off\ from\ m\ and\ passes\ through\ i\ to\ j, \forall i, j \in V, m \in J \\ 0, others \end{cases};$$

Decision variables $y_{ij} = \begin{cases} 1, the\ truck\ goes\ through\ i\ to\ j, \forall i, j \in J' \\ 0, others \end{cases}$;

Auxiliary decision variables $f_i > 0, \forall i \in J$, avoiding truck sub-loop. Auxiliary decision variables $t_{ij}^{truck} \geq 0, \forall i, j \in J'$ present the time required for the truck to travel from i to j. Auxiliary decision variables $s_i^{truck} \geq 0, \forall i, j \in J'$ present the time point of truck arrives i. Auxiliary decision variables $u_{im}, \forall i \in V, m \in J$, avoiding drone sub-loop. Auxiliary decision variables $w_{ij} \geq 0, \forall i, j \in V, m \in J$ present the residual load of the drone from i to j. Auxiliary decision variables $t_{ij}^{drone} \geq 0, \forall i, j \in V$ present the time required for drone from i to j.Auxiliary decision variable $b_{im} > 0, \forall i \in V, m \in J$ represents the remaining battery capacity of the drone serving the disaster site i after the truck arrives at cluster center m. Auxiliary decision variables $s_{im}^{drone} > 0, \forall i \in V, m \in J$ represent the time node when the drone arrives at the disaster site i after the truck arrives at the cluster center m. Auxiliary decision variables $T_m > 0, m \in J$ represent the time node after the truck reaches the cluster center m. The research model assumes the following conditions: 1) the number of drones is limited due to the limited capacity of the truck, and all drones are homogeneous; 2) the emergency material demand of each disaster site is known and only served by one drone once; 3) the drones can bear the emergency material weight required by the disaster site, without overloading and unpacking; 4) the drones are launched and retrieved from the truck, and return to the truck after one distribution, and replace the back-up battery; 5) the drones are not considered the service time of the disaster site, and the drones fly at a stable speed, assuming fixed air and gravity fluid density; 6) the psychological trauma generated by the inequity phenomenon at each disaster site can be quantified by the economic loss (Pérez-Rodríguez & Holguín-Veras 2016).

3.2 Mixed Integer Programming Model

The energy consumption estimation model of drones is assumed to be a quasi-linear relationship function between power P and load w (Jeong et al., 2019). An energy consumption estimation formula for drone emergency material delivery tasks in humanitarian rescue scenarios is constructed. The drone flight time is introduced, and then the power consumption of the drone from the flight process e_{ij} is expressed as:

$$e_{ij} = P\big(w_{ijk}\big)\, l_{ij}/v = \big(\beta_0 + \beta_1 w_{ijk}\big) l_{ij}/V_{drone} \tag{1}$$

Among them, β_0 and β_1 are the relevant parameters of power function after linearization, w_{ijk} is the total weight of the remaining materials during the delivery of the drone k from i to j, l_{ij} is the distance between i and j, V_{drone} is the drone's stable flight speed. When the drone battery capacity E is fixed, the maximum flight distance of the drone R_x can be determined by the formula above, which can be expressed as:

$$R_x = \frac{\eta E * V_{drone}}{2(\beta_0 + \beta_1 * W)} \tag{2}$$

Among them, η is the drone battery energy consumption parameters, and E is the drone battery capacity. To approximately describe the psychological trauma caused by the lack of emergency supplies in each disaster site, referring to the linearization processing of the deprivation cost function by Biswal et al. (2018), then the deprivation cost DC_i with penalty cost ω caused by disaster sites i can be expressed as:

$$DC_i = \sum_{d \in D} \sum_{m \in J} [\omega q_{id} s_{im}^{drone} + \omega(Q_{id} - q_{id}) * T_m]\,, \forall i \in N \tag{3}$$

Among them, s_{ik} indicates the time point after the drone k reaches disaster site i, and $T_m$is the complete process time of the distribution task. The deprivation cost of disaster sites is composed of two parts: one is the cost of psychological trauma suffered by the disaster victims from waiting until receiving the emergency materials $\omega q_{id} s_{im}^{drone}$, and the other is the cost of psychological trauma accumulated by the disaster victims who still do not receive the required emergency materials after the entire process of distribution task $\omega(Q_{id} - q_{id}) * T_m$. To reflect the fairness principle of humanitarian relief, the "relative deprivation cost" is proposed to measure the degree of psychological trauma differentiation of the victims in different disaster-affected sites due to the failure to receive emergency response materials in time, and it is used as the difference index to measure the fairness of distribution programs. Therefore, the relative deprivation cost RDC_i of the disaster-affected site i can be expressed as:

$$RDC_i = DC_i - \min(DC_i)\,, \forall i \epsilon N \tag{4}$$

The objective function is as follows:

$$min\left\{ C_{truck} \sum_{i \in J'} \sum_{j \in J'} l_{ij}\, y_{ij} + C_{drone} \sum_{i \in V} \sum_{j \in V} \sum_{m \in J} l_{ij} x_{ijm} + (L + R) \sum_{i \in J} \sum_{j \in N} \sum_{m \in J} x_{ijm} + \sum_{i \in N} RDC_i \right\} \tag{5}$$

The total cost in Eq. (5) includes the truck path cost, the drone path cost, the fixed cost of the drone launch and reception, and the relative deprivation cost to measure fairness. The constraints of the model are as follows: The formula (6) represents the relative deprivation cost of each disaster site, which measures the fair difference. The formula (7) represents the deprivation cost of each disaster site disaster victim, which is caused by not receiving emergency supplies.

$$RDC_i = DC_i - \min(DC_i)\,, \forall i \epsilon N \tag{6}$$

$$DC_i = \sum_{d \in D} \sum_{m \in J} [\omega q_{id} s_{im}^{drone} + \omega(Q_{id} - q_{id}) * T_m]\,, \forall i \in N \tag{7}$$

Formula (8) indicates that the round-trip distance from any disaster site to a truck stop is in the flight range of a drone.

$$l_{im} = \sqrt{(A_i - a_z)^2 + (B_i - b_z)^2} \le R_x, \forall z \in J, \exists i \in N \tag{8}$$

The formula (9-10) indicates that any truck stop can be divided into paths: the truck arrives at each stop once and leaves after the drone completes the task. The formula (11) guarantees that the truck must return to the distribution center to avoid generating sub-circuits. The formula (12) indicates that the truck capacity is limited and limits the maximum number of drones.

$$\sum_{i \in J'} y_{ij} = 1, \forall i \in J', i \neq j \tag{9}$$

$$\sum_{j\in J'} y_{ij} = 1, \forall i \in J', i \neq j \tag{10}$$

$$f_i - f_j + (n+2) * y_{ij} \leq n+1, \forall i,j \in J \tag{11}$$

$$\sum_{j\in N} x_{mjm} \leq K \tag{12}$$

Formula (13-14) indicates that each disaster site is evenly distributed to the path: the disaster site is served once by the drone, and the drone must leave after serving. Formula (15) ensures that the path flow of the drone is balanced: each disaster site has access to the other. Formula (16-17) ensures that each disaster site only belongs to a truck stop point service and excludes other situations. Formula (18-19) ensures that the weight of the drone is reduced during the flight process while avoiding the drone sub-loop.

$$\sum_{m\in J}\sum_{j\in V} x_{ijk} = 1, \forall i \in N \tag{13}$$

$$\sum_{m\in J}\sum_{i\in V} x_{ijk} = 1, \forall j \in N \tag{14}$$

$$\sum_{i\in V} x_{ijm} = \sum_{i\in V} x_{jim}, \forall j \in V, m \in J \tag{15}$$

$$x_{jim} = 0, \forall i \in N, j \in J, m \in J, j \neq m \tag{16}$$

$$x_{ijm} = 0, \forall i \in N, j \in J, m \in J, j \neq m \tag{17}$$

$$u_{jm} \geq u_{im} + w_j - M\left(1 - x_{ijm}\right), \forall i \in V, j \in N, m \in J \tag{18}$$

$$w_i \leq u_{im} \leq W, \forall i \in V, m \in J \tag{19}$$

The formula (20-21) represents the dynamic counterweight constraint during the drone distribution process, and the formula (22-24) represents the drone battery capacity constraint.

$$w_{ij} \leq W * \sum_{m\in J} x_{ijm}, \forall i,j \in V, i \neq j \tag{20}$$

$$\sum_{j\in V} w_{ji} - \sum_{j\in V} w_{ij} = w_i, \forall i \in N \tag{21}$$

$$0 < b_{im} \leq \eta E, \forall i \in V, m \in J \tag{22}$$

$$b_{mm} = \eta E * \sum_{j\in N} x_{mjm}, \forall m \in J \tag{23}$$

$$b_{jm} \geq b_{im} - e_{ij} - \eta E\left(1 - x_{ijm}\right), \forall i,j \in V, i \neq j, m \in J \tag{24}$$

The formula (25-28) indicates that the truck arrives at each truck stop in sequence constraints.

$$s_O^{truck} = T_{start} \tag{25}$$

$$t_{ij}^{truck} = \left(l_{ij}/V_{truck}\right) * y_{ij}, \forall i,j \in J' \tag{26}$$

$$s_j^{truck} \geq s_m^{truck} + t_{mj}^{truck} - M\left(1 - y_{mj}\right), \forall m \in J\backslash\{n+m\}, j \in J \tag{27}$$

$$s_j^{truck} \leq s_m^{truck} + t_{mj}^{truck} + M\left(1 - y_{mj}\right), \forall m \in J\backslash\{n+m\}, j \in J \tag{28}$$

The formula (29-31) represents the time sequence constraints of the drone reaching the disaster site.

$$s_{mm}^{drone} = T_{start}, \forall m \in J \tag{29}$$

$$t_{ij}^{drone} = (l_{ij}/V) * \sum_{m \in J} x_{ijm}, \forall i,j \in V, i \neq j, m \in J \tag{30}$$

$$s_{jm}^{drone} \geq s_{im}^{drone} + t_{ij}^{drone} - M(1 - x_{ijm}), \forall i,j \in V, i \neq j, m \in J \tag{31}$$

The formula (32-37) represents the decision variables of the model.

$$(a_z, b_z), \qquad \forall z \in J \tag{32}$$

$$T_m = max(s_{im}^{drone}) > 0, \forall i \in N, m \in J \tag{33}$$

$$f_i > 0, \forall i \in J; s_i^{truck} \geq 0, \forall i \in J' \tag{34}$$

$$y_{ij} \in \{0,1\}, t_{ij}^{truck} \geq 0, \forall i,j \in J' \tag{35}$$

$$x_{ijm} \in \{0,1\}, w_{ij} \geq 0, t_{ij}^{drone} \geq 0, \forall i,j \in V, m \in J \tag{36}$$

$$u_{im} \geq 0, b_{im} > 0, s_{im} > 0, \forall i \in V, m \in J \tag{37}$$

3.3 Double-Level Programming Mathematical Model

Benders Decomposition was proposed by BnnoBRs (1962) and used to solve large-scale mixed integer programming problems. The basic idea is to decompose a large-scale problem into a central problem and sub-problem by fixing the value of complicating variables and adding optimal cuts or feasible cuts to the main problem through the sub-problem (Poojari & Beasley, 2009; Alfandari et al., 2022), the main problem and sub-problem, respectively, and finally achieve the convergence of the solution. The mixed integer programming model of this problem is analyzed. It is found that the problem can be transformed into a double-level programming problem when the truck stops (a_z, b_z) is fixed. The upper-level problem is a location-truck routing problem (LTRP), which determines the locations of the stops that the trucks need to traverse and the optimal traversal routes. The lower-level problem is a multi-depot drone routing problem (MDDRP), which determines the optimal routes for drones to distribute goods from the stops to the disaster sites. The decision-making process of the problem is shown in Fig. 2. Fig. 2 (a) to Fig. 2 (b) is the location process of the truck stops. Fig. 2 (b) to Fig. 2 (c) is the decision-making process of the truck optimal distribution path, which will determine the order of truck distribution: trucks from the distribution center traverse all the truck stops and finally return to the distribution center. When the truck stops (a_z, b_z) are fixed, the process is the decision-making process of the upper-level problem. Fig. 2 (c) to Fig. 2 (d) is the decision-making process of the drone dispatching and distribution; in this process, after the truck reaches a stop point, the drone is released to carry out the material distribution task at the disaster-affected site, and when all the drone distribution tasks are finished, the truck starts to go to the next stop point to continue the drone dispatching and material distribution work. When the truck stops (a_z, b_z) are fixed, the process is the decision-making process of the lower-level problem.

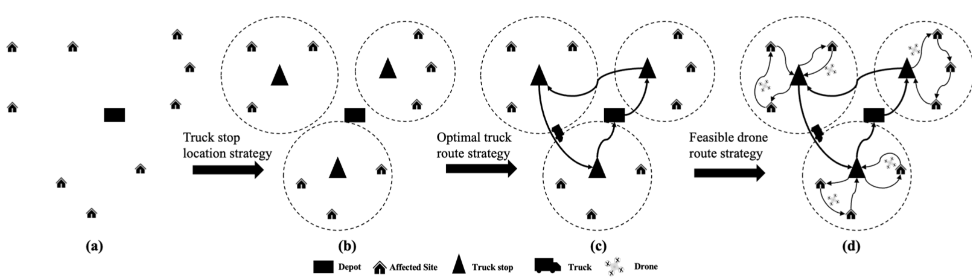

Fig. 2. Schematic diagram of the decision-making process

The mathematical model of the upper-level problem LTRP is:

$$min\left\{C_{truck} \sum_{i \in J'} \sum_{j \in J'} l_{ij}\, y_{ij}\right\} \tag{38}$$

subject to:

(8) ~ (12); (25) ~ (28); (33) ~ (35)

The mathematical model of the upper-level problem MDDRP is:

$$min\left\{\sum_{i\in V}\sum_{j\in V}\sum_{m\in J} l_{ij}x_{ijm} + (L+R)\sum_{i\in J}\sum_{j\in N}\sum_{m\in J} x_{ijm} + \sum_{i\in N} RDC_i\right\} \quad (39)$$

subject to:

(6) ~ (7); (13) ~ (24); (29) ~ (31); (36) ~ (37)

4. Two-Stage Heuristic

To solve the truck-drone joint path optimization problem, a two-stage heuristic algorithm TD-TSH was developed, which was inspired by the bi-level programming model and combined with the Greedy algorithm with K-means (K-means GA) and the adaptive large neighborhood search (ALNS). In TD-TSH, K-means GA is used to solve LTRP, and ALNS is used to solve MDDRP. The solution to the problem includes the location of the truck stop, the route of the truck, and the distribution scheme of the drone. The TD-TSH designed in this paper is shown in Fig. 3.

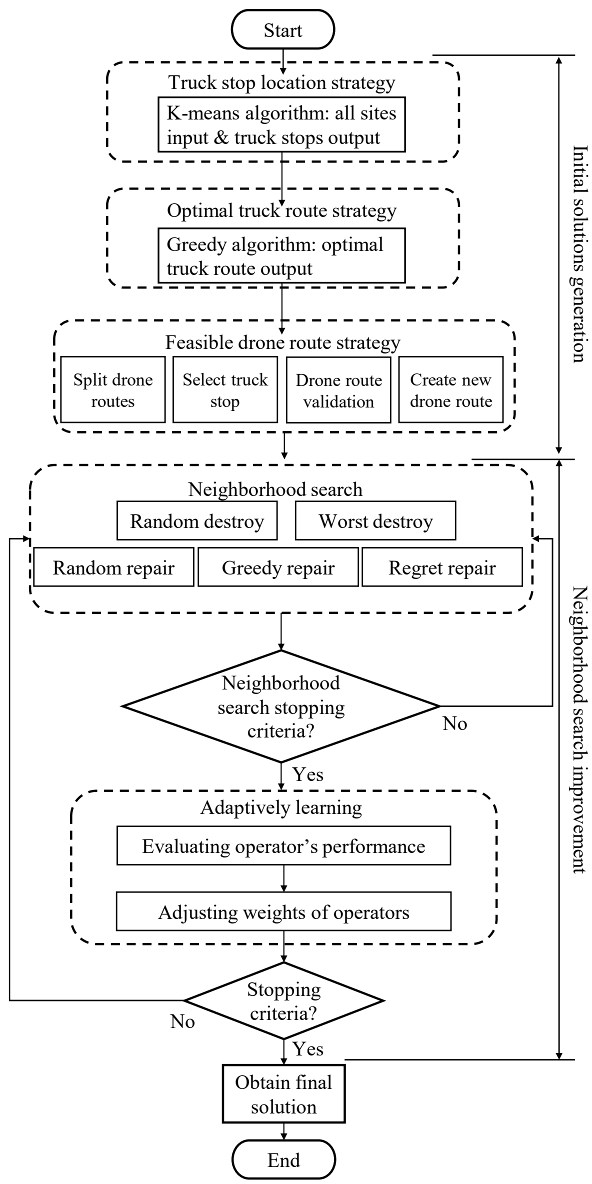

Fig. 3. Schematic diagram of TD-TSH

In the initial solution generation phase, following the characteristics of the solution, the K-means GA is used to solve the LTRP, adding heuristic rules based greedy strategy to solve the truck route. The ALNS is used to solve the MDDRP. In the neighborhood search improvement phase of searching for the optimal solution in the field of iterative optimization, a variety of destroy and repair operators based on the characteristics of the problem are used to explore the possible solution space.

4.1 Initial Solution Generation

4.1.1 K-Means GA For LTRP

The K-Means GA mainly solves the location of truck stops and the optimal delivery route. K-Means GA mainly includes two modules: truck stop location strategy and optimal truck route strategy.

Truck stop location strategy: (1) Pick up random K points from the set of affected points $N = \{1,2,\cdots,n\}$ as the initial truck stop. The parameters k are generated first through the "elbow method"; further adjustments are made through the indicator k to obtain a more appropriate K. R_x presents the maximum allowable straight line round trip Euclidean distance between the disaster site and the cluster center.

(2) Calculate the Euclidean distance from each disaster site to the initial truck stop in the set of disaster sites $N = \{1,2,\cdots,n\}$, and assign it to the nearest cluster. Then, calculate the center of gravity of each cluster as a new truck stop and repartition which stop the disaster site belongs to. Repeat this process until the iterative results meet the termination conditions. Termination conditions: There is no redistribution of affected points to different truck stops, no change in truck stops, and least square error.

Optimal truck route strategy: Through the above strategies, we can get the set of the distribution center, and the truck stops J', calculate the distance matrix of all nodes in the set J', generate a truck TSP path with minimum driving distance according to the greedy strategy, this TSP path from the distribution center, through all the truck stops, and finally back to the distribution center.

4.1.2 ALNS For MDDRP

The ALNS is mainly used to solve the optimal distribution scheme of drones. The path of the drone is encoded by real number coding. The n affected points in the damaged area are designed as a set with n numbers encoded. The random distribution order of the drone to each affected point is represented by a random arrangement from 1 to n natural numbers. For all the disaster sites, the distribution scheme is a real number encoded path set; all the paths in the set will traverse all the disaster sites.

(1) Split drone routes

A TSP path is generated randomly to traverse all the affected points without considering the starting point, the recovery point, the load, and the energy consumption of the drone. For the generated TSP path, according to the greedy strategy, determine whether the accumulated weight of emergency supplies distributed by each disaster site meets the maximum load capacity of the drone. If the weight of the material distributed by the next disaster site exceeds the residual load capacity of the drone, a new path is split from the current disaster site position, the number of drones is increased, and the solution set S containing several sub-paths of the drones is generated.

(2) Select truck stop

For each drone sub-path in the solution set S, according to the principle of "distance minimization", the closest truck stop point of the first disaster site in the ion path is selected as the drone's sending point and reclaiming point, and the solution set S is updated. Then, all drone sub-paths can be assigned to truck stops. The solution set S is analyzed to determine whether the number of drones needed exceeds the maximum capacity of the truck. If the number exceeds the maximum capacity of the truck, the operation is terminated in advance, and no solution is output.

(3) Drone route validation

For each drone sub-path in the solution set S, the dynamic load data of each path when the drone reaches each disaster site is calculated: the weight of the material distributed by each disaster site in the known path is respectively $[w_1, w_2, w_3, \ldots, w_n]$, and the accumulated weight $[w_n + w_{n-1} + w_{n-2} + \ldots + w_1, w_n + w_{n-1} + w_{n-2} + \ldots + w_2, \ldots, w_n + w_{n-1}, w_n]$ of the emergency material carried by the drone when it reaches the current disaster site is obtained by adding them in reverse order, then the power consumption $\sum_{i \in V} \sum_{j \in V} (\beta_0 + \beta_1 w_{ijk}) l_{ij} / v * x_{ijk}$ of each drone sub-path in the whole flight process is calculated. If the total energy consumption is less than the maximum releasable energy of the drone battery, the path is true, and if the total energy consumption is more than the maximum releasable energy of the drone battery, the path is not valid, and an unfeasible path set R is generated. Since the set R is a subset of the solution set S, the subset R of the solution set is S eliminated to obtain an updated set S' of feasible paths.

(4) Create new drone routes

For each path in the path set R, the "tail customer judgment method" is used to eliminate the tail disaster sites until the path to eliminate the disaster sites is in line with the maximum releasable energy requirements of the drone battery. For the eliminated disaster sites, several new paths are generated, and the path sets R is updated based on the load and battery capacity consumption of drones. The path set R is merged into the solution set S', and the solution set S' is the initial feasible solution set of the ALNS.

4.2 Neighborhood Search Improvement

In this paper, we propose two kinds of destroy operators, three kinds of repair operators, and a drone path adjustment strategy to generate a feasible neighborhood solution. Given an integer θ, firstly, a removal operator is randomly used to remove θ damaged point codes from the current solution, and then a repair operator is randomly used to reinsert the removed damaged point codes to form a new drone distribution scheme. The path adjustment strategy is based on the dynamic energy consumption characteristics of the drone battery, and the adjustment of disaster sites in the path of the drone is introduced to optimize the neighborhood solution. Here are two destroy operators:

(1) Random destroy operator
Randomly select θ affected point codes to remove from the current solution. The random destroy operator is random, and its purpose is to expand the search range of the neighborhood solution and avoid getting into the local optimum. θ depends on the number of disaster sites in the current solution, where $\theta \in [1, n]$.

(2) Worst destroy operator
Given the current solution S and a disaster site code n, F' is the target function value after removing the disaster site code from the current solution, $F(S)$ is the target function value of the current solution, $\Delta(n, S) = F(S) - F'$. The destroy operator starts by removing a disaster site code until removing θ disaster site codes in turn. The basis of removal is that $\Delta(n, S)$ is the largest after removing the disaster site code n. θ depends on the number of disaster sites in the current solution, where $\theta \in [1, n]$. After the destruction operator operation is completed, three repair operators are used to reinsert the deleted disaster site codes into the current solution for drone path reconstruction:

(1) Random repair operator
Randomly selected θ locations are inserted into the θ removed affected point codes. The random destroy operator is random, and its purpose is to expand the search range of the neighborhood solution and enrich the diversity of the solution.

(2) Greedy repair operator
According to the greedy strategy, for each disaster site code, let $\Delta C(n, u)$ present the increased cost of the disaster site code n inserted into the u^{th} position of the original path and sequentially select the minor $\Delta C(n, u)$ corresponding position to insert until all the disaster sites are inserted.

(3) Regret repair operator
Let $C(n)$ present the difference between the cost calculated after the disaster site code n is inserted into the best insertion position and the cost calculated after the second-best insertion position is recorded. The larger $C(n)$ of affected point n, the greater the benefit of not inserting the optimal location at the current time and then inserting it into other locations. For each affected point code, select the most significant $C(n)$ position in turn to insert until all the affected points are inserted. Compared with the greedy operator, this operator belongs to the global optimal insertion matching operator, which enhances the optimization ability of the algorithm, but it needs more search time.

4.3 Path Adjustment of Drones

For the solution set generated after the neighborhood search operation and the load change of the drone caused by the operation, execute the $Drone\ routes\ validation$ and $Create\ new\ drone\ routes$, adjust all the infeasible paths to feasible paths, and update the evolution solution set.

4.4 Acceptance criteria for solutions

In this study, the solution acceptance criterion of the simulated annealing algorithm is introduced into the iterative local search algorithm, which can accept the poor solution with a certain probability, thus enhancing the probability of jumping out of the local optimum and enhancing the ability to search for the optimal solution. The strategy is as follows: Suppose the local optimal solution S' of the current solution S is obtained by large-scale neighborhood search; when S' is inferior, S' is accepted with certain probability.

5. Numerical Experiments and Analysis

In order to verify the effectiveness of the TD-TSH, a series of numerical experiments were designed and tested, and the improved algorithm was based on Augerat (https://neo.lcc.uma.es/vrp/vrp-instances/capacitated-vrp-instances). The classical CVRP example set presented in this paper is suitable for the realistic situation of the research model in this paper: the emergency material type is set to 1, which has no heterogeneity; the material demand weight multiplied by 0.1 is suitable for the drone load, the unit takes kg. The stable flight speed of the drone is set to 10 km/h, and the parameters in the energy consumption function and deprivation cost function are set to $\beta_0 = 1.58, \beta_1 = 0.217$ (Zhu et al., 2019), $\omega = 100$ (Biswal et al., 2018). TD-TSH and ACO are implemented by Python programming, and the compiler is Python 3.9. The computer configuration is Intel Core i5-7200U, CPU 2.50GHz, 4GB memory. The MIP model is calculated by CPLEX12.8.

5.1 Taguchi Analysis

The parameters of the algorithm have a particular impact on the performance of the algorithm, and suitable parameters can improve the performance of the algorithm to a certain extent, so determining a reasonable value of the parameters is very important. Taguchi design is a parameter design method that originated from the field of quality management, with the aim to determine the optimal level of parameters with the least number of tests. With its superior reliability and reproducibility, simple analysis has been widely used (Soleimanin et al., 2017). Taguchi method mainly measures the parameters by the signal-to-noise ratio; the more significant the signal-to-noise ratio, the more reasonable the corresponding parameter settings. TD-TSH uses the objective function for minimizing the system cost, and the corresponding formula is:

$$\frac{S}{N} = -10 * log_{10}(\sum_{t=1}^{n}(F_t^2 /n)) \tag{40}$$

Here, n is the execution times of the algorithm at the level of each parameter, F_t is the response value, that is, the objective function value of the t^{th} experiment.

The parameters of TD-TSH are the maximum random destroy proportion rd_{max}, the minimum random destroy proportion rd_{min}, the maximum worst destroy quantity wd_{max}, the minimum worst destroy quantity wd_{min}, the regret destroy quantity $regret_n$, the first score value r_1, the second score value r_2, the third score value r_3, the weight attenuation proportion rho, the annealing rate phi, the total number of inner and outer cycles $epochs$. According to the previous experience and the algorithm coding features set, rd_{max} is 0.2, and rd_{min} is 0.1, wd_{max} is 6, wd_{min} is 1, $regret_n$ is 1, r_1 is 30, r_2 is 20, r_3 is 10. The weight attenuation ratio, annealing rate, and the number of inner and outer loop iterations were optimized by the Taguchi analysis method to determine the optimal value. Considering orthogonal experimental design optimization, each parameter takes three levels: rho is taken from {0.3,0.4,0.5}, phi is taken from {0.7,0.8,0.9}, and $epochs$ taken from $\{10 * 10, 15 * 15, 20 * 20\}$. Taguchi analysis was performed by using $L9$ type orthogonal test table, and five experiments were repeated for each level combination. Table 1 gives the results of the Taguchi orthogonal experiment, the total cost of each scheme, and the corresponding signal-to-noise ratio and mean.

Table 1
Taguchi Analysis

	rho	phi	epoch	Run-1	Run-2	Run-3	Run-4	Run-5	Avg.	S/N
1	0.3	0.7	100	3529.17	3657.62	3341.69	3465.31	3460.01	3490.76	-70.862
2	0.3	0.8	400	3285.19	3345.95	3420.28	3347.22	3295.09	3338.746	-70.473
3	0.3	0.9	225	3386.5	3488.37	3531.2	3354.17	3420.69	3436.186	-70.723
4	0.4	0.7	400	3451.6	3324.67	3325.66	3276.57	3319.92	3339.684	-70.475
5	0.4	0.8	225	3256.44	3442.69	3412.56	3343.47	3466.68	3384.368	-70.592
6	0.4	0.9	100	3496.51	3734.65	3623.57	3757.57	3501.78	3622.816	-71.185
7	0.5	0.7	225	3380.38	3345.13	3405.36	3287.74	3461.11	3375.944	-70.569
8	0.5	0.8	100	3415.09	3533.66	3585.82	3471.56	3590.78	3519.382	-70.931
9	0.5	0.9	400	3339.44	3333.12	3473.22	3333.65	3368.84	3369.654	-70.553

The figure below shows the main effect graphs of the average signal-to-noise ratio and the main effect graphs of the average signal-to-noise ratio for each parameter at different levels. From Fig. 4, we can see that when the weight attenuation ratio is 0.5, the annealing rate is 0.7, and the number of inner and outer iterations is 400, the corresponding signal-to-noise ratio is the largest, and the corresponding average total cost is also the smallest, as shown in Fig. 5. Based on the above analysis, the parameters of the algorithm are set as shown in Table 2.

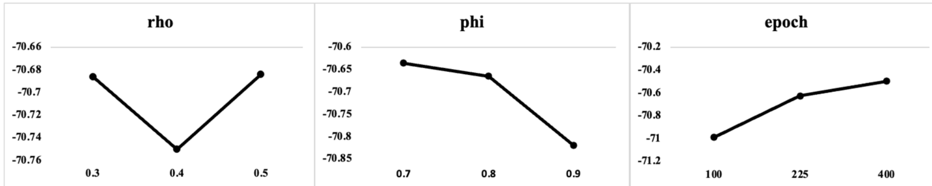

Fig. 4. Principal effect diagram of signal-to-noise ratio for orthogonal experiment

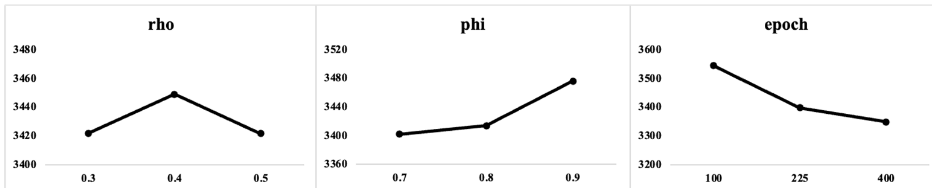

Fig. 5. Main effect diagram of the mean value for the orthogonal experiment

Table 2
Algorithm Parameter Settings

rd_{max}	rd_{min}	wd_{max}	wd_{min}	$regret_n$	r_1	r_2	r_3	rho	phi	$epoch$
0.2	0.1	6	1	1	30	20	10	0.5	0.7	400

5.2 Analysis of Optimization Results

The optimization results of TD-TSH are analyzed by taking "Set A-N36" as an example. The optimal truck-drone joint path planning obtained by the algorithm is shown in Figure 6. We know that: (1) The disaster sites in the whole disaster-affected area are divided into four distribution areas. The truck carries drones and rescue materials from the emergency center and carries out material distribution plans one by one for each disaster-affected point in each distribution area. (2) All truck stops are traversed once by the truck, and the material distribution tasks in the four disaster-affected areas are all completed by the drone. (3) The disaster-affected sites in the same disaster-affected area are all distributed by the same drone. The path planning of multi-drones is less cross and circuitous. (4) All drones start distribution from the nearest truck stop. This shows that K-means GA can reasonably cluster the disaster sites, ALNS can reasonably plan the truck-drone joint distribution path according to the actual situation and minimize the total cost of the distribution system.

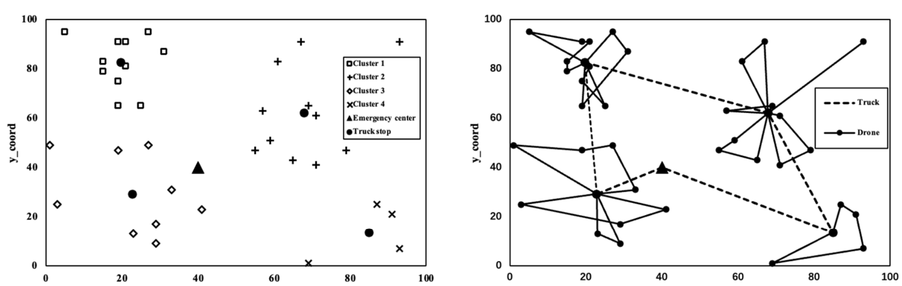

Truck Route	Depot -> 38 -> 36 -> 37 -> 39 -> Depot			
Drone 1 Route	38 -> 10 -> 7 -> 38	36 -> 18 -> 21 -> 27 -> 36	37 -> 3 -> 12 -> 37	39 -> 2 -> 35 -> 8 -> 15 -> 39
Drone 2 Route	38 -> 20 -> 26 -> 16 -> 38	36 -> 22 -> 32 -> 30 -> 17 -> 13 -> 36	37 -> 4 -> 37	
Drone 3 Route	38 -> 5 -> 25 -> 11 -> 1 -> 38	36 -> 29 -> 33 -> 24 -> 36	37 -> 31 -> 19 -> 37	
Drone 4 Route	37 -> 28 -> 9 -> 14 -> 37			
Drone 5 Route	37 -> 34 -> 23 -> 6 -> 37			

Fig. 6. Schematic diagram of optimal joint path planning scheme

5.3 Comparative Analysis of Algorithms

In this paper, CPLEX is used to obtain the exact solution of a small-scale case, and the validity and accuracy of the hybrid algorithm are compared. For large-scale cases, the comparison with the ACO, which has a better solution effect, is carried out, and the advancement and universality of TD-TSH are further verified. The exact solutions of small-scale examples are compared and analyzed. When the problem scale and constraints are complex, CPLEX cannot solve the MDDRP under bilevel programming. Therefore, a small-scale example ($N = 23,22,21,20,19,16$) is set to compare with it. The solution results are shown in Table 3, where $GAP = (Sol(TD - TSH) - Sol(CPLEX)) * 100\%$. The value with an asterisk indicates that CPLEX does not find the optimal solution within the prescribed 3600 seconds; only the feasible solution is obtained. From Table 3, for small-scale examples, the results of TD-TSH are close to the exact solution of CPLEX; the difference is only 0~3.36%. In the solution time, TD-TSH is significantly shorter, the average is less than 1.24s, and the average time is reduced by 99.20% compared with CPLEX. With the increase in computational complexity, the solution time of the CPLEX solver increases sharply, and it is more difficult to find a better solution. Therefore, compared with the exact solution method, using TD-TSH to solve MDCVRP has some time advantages while maintaining accuracy and effectiveness.

Table 3
Comparison and Analysis of Exact Solutions for Small-Scale Examples

Instance	CPLEX Best Sol.	TD-TSH Best Sol.	GAP	CPLEX Time(s)	TD-TSH Time(s)	Reduction Rate
Set P-N=16	483.924	484.336	0.09%	35.28	2.96	91.61%
Set P-N=19	556.575	556.578	0.00%	675.46	9.99	98.52%
Set P-N=20	533.212	551.126	3.36%	208.78	9.69	95.36%
Set P-N=21	574.286*	581.49	1.25%	**3600**	14.29	99.60%
Set P-N=22	535.975	548.286	2.30%	328.89	12.79	96.11%
Set P-N=23	591.886*	608.342	2.78%	**3600**	17.71	99.51%
Avg.	-	-	-	1408.07	11.24	99.20%

The comparative analysis of large-scale algorithms is carried out. At present, in the MDDRP problem, the ACO proposed by Dorigo and Gambardella (1997) has a better solution effect and has obtained a higher recognition as a comparative algorithm for the study. The number of customers N of large-scale example sets Set A and Set P is taken within $[32, 101]$. The two algorithms run ten times separately for each instance, and the solution results are shown in Table 4. $Best$ is the optimal solution for ten times of operation results. $Worst$ is the worst solution for ten times of operation results, $Avg.$ is the average result for ten times of operation, $GAP = (Avg.(TD-TSH) - Avg.(ACO))/Avg.(TD-TSH) * 100\%$. From Table 4, it can be seen that according to the value of $Avg.$, the average cost of the total system cost obtained by the TD-TSH in all the instances is better than that obtained by the ACO, the maximum savings is 5.75%, and the minimum savings is 0.34%, which indicates that the TD-TSH can effectively reduce the total system cost of truck-drone joint transportation.

Table 4
Comparative Analysis of Large-Scale Computational Examples

Instance	TD-TSH			ACO			GAP
	Best	Worst	Avg.	Best	Worst	Avg.	
Set A-N=32	3245.74	3365.86	3299.32	3351.12	3451.18	3407.26	3.27%
Set A-N=36	2834.31	2995.62	2913.63	2863.17	2984.51	2926.06	0.43%
Set P-N=40	2949.80	3038.33	3003.00	2994.58	3095.82	3062.74	1.99%
Set A-N=44	4035.13	4400.45	4188.02	4371.35	4484.06	4428.91	5.75%
Set P-N=45	3439.19	3511.50	3479.46	3499.46	3612.09	3546.23	1.92%
Set A-N=53	4442.17	4595.32	4506.49	4598.37	4850.57	4738.33	5.14%
Set P-N=55	4514.89	4661.16	4582.51	4624.38	4715.57	4668.76	1.88%
Set A-N=64	5473.28	5744.73	5636.18	5547.20	5776.50	5658.93	0.40%
Set P-N=70	6362.69	6760.98	6487.67	6529.98	6666.01	6595.57	1.66%
Set P-N=76	6659.54	6774.98	6729.22	6640.81	6892.55	6752.05	0.34%
Set A-N=80	6739.37	6836.45	6794.97	6925.10	6968.45	6945.82	2.22%
Set P-N=101	7286.35	7309.84	7298.10	7472.20	7605.81	7539.01	3.30%

The efficiency of the TD-TSH is further tested by the example "Set A-N36". From Table 4, we can see that the average optimization result of ACO is 2926.06, while the average optimization result of TD-TSH is 2913.63, which is better.

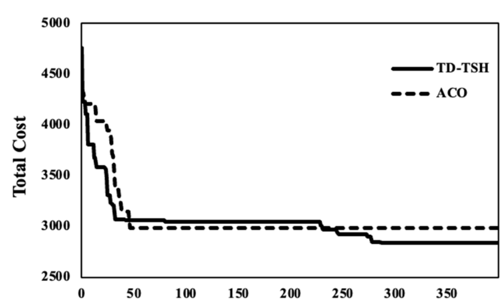

Fig. 7. Schematic diagram of the iterative process of TSH and ACO optimal results

Fig. 7 is the optimal result iteration curves of TD-TSH and ACO. TD-TSH uses heuristic rules to construct the initial solution. At the beginning of the iteration, the total cost of the truck-drone distribution system is optimized to a near-optimal position. However, ACO converges quickly, but it is still far from TD-TSH. TD-TSH optimizes the solution space of the drone path rapidly by judging the load and battery capacity of the drone in the early stage of operation. TD-TSH introduces two kinds of destroy operators, which make the search space more extensive and more directional, not only enhancing the ability of optimization but also significantly improving search efficiency. In addition, the greedy repair operator is introduced to accelerate the search process of the neighborhood feasible solution, and the balance between search quality and search time is achieved by alternately calling the optimal repair operator and the maximum contribution repair operator. However, ACO is too blind in each search and does not make any judgment on the infeasible solution in the solution space. The optimization effect could be more apparent, and the premature convergence phenomenon is easy to occur. The proposed TD-TSH can effectively improve the convergence efficiency and effectiveness of the solution.

Furthermore, to observe the variation amplitude of each cost index with the change of the drone battery capacity E, referring to the experimental results of five groups of examples, taking E as the horizontal axis, the three cost indexes as the vertical axis are plotted respectively, as shown in Figure 8. From the figure, with the increase of E, the total cost of the system decreases gradually, which shows that the increase in battery capacity will affect the reduction of the total cost of the system to a certain extent. The economic cost of truck-drone transportation and the relative deprivation cost of fairness were observed, and the economic cost decreased gradually with the increase of E, but the relative deprivation cost increased gradually. This shows that the increase in the battery capacity of drones will lead to the reduction of economic costs but also will lead to the increase of the relative cost of deprivation. The endurance capability of drones is an essential factor in reducing economic costs, but it may lead to the occurrence of unfair phenomena. When the drone battery capacity increases, the drones tend to rescue more disaster-affected points, compared with more drones at the same time, material ration, to some extent, will temporarily suspend some of the disaster-hit points' material ration, which is not conducive to alleviating the trauma of the victims. Each drone distribution path will be longer, thus conducive to reducing the number of drones initiated, so the overall system cost is reduced.

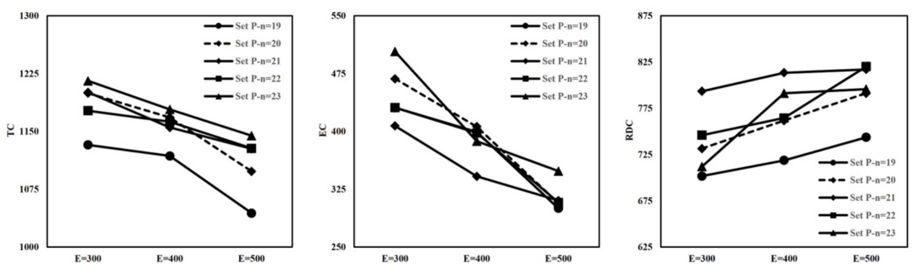

Fig. 8. Variation range of each cost index with battery capacity E of drone

Through the above analysis, it can be found that only based on the economic cost of the drone emergency material deployment decision, although the number of drones and the total cost of the system can be well controlled, in the humanitarian relief of the more critical victims of psychological trauma, not necessarily achieve good results. When making decision plans, we should not only pursue the improvement of drone battery capacity. However, drones with higher endurance levels can undertake more distribution tasks at disaster sites to some extent but may cause unfair phenomena. Of course, to the extent that the economic cost allows, the smaller the fairness threshold based on the total relative deprivation cost is, the better. Therefore, considering the economic cost and the relative deprivation cost as the crucial objectives of decision-making, the deployment scheme of drones can get result in relative economic fairness.

6. Conclusion

In this paper, the total cost of truck-drone transportation and the relative deprivation cost of fairness are considered as the objectives. The allocation problem of emergency supplies for truck-drone joint transportation with dynamic energy constraints and fairness is studied, and the corresponding mixed integer programming model MIP is constructed. To solve the model, a two-stage heuristic algorithm TD-TSH was designed, and many numerical experiments were conducted to verify the effectiveness and stability of the algorithm. TD-TSH performs well in small-scale cases and is stable in large-scale cases. Further study found that the battery capacity of drones affects the total cost of the distribution process by influencing the flight time of drones, and the impact of emergency material allocation planning decisions can not be ignored. The truck-drone joint path planning scheme has practical significance and can provide a valuable reference for building a fair and efficient drone emergency rescue system.

Conflicts of interest

The authors declare that they have no conflicts of interest to report regarding the present study.

References

Agatz, N., Bouman, P., & Schmidt, M. (2018). Optimization approaches for the traveling salesman problem with drone. *Transportation Science*, *52*(4), 965-981.

Alfandari, L., Ljubić, I., & da Silva, M. D. M. (2022). A tailored Benders decomposition approach for last-mile delivery with autonomous robots. *European Journal of Operational Research*, *299*(2), 510-525.

Balcik, B., & Beamon, B. M. (2008). Facility location in humanitarian relief. *International Journal of logistics*, *11*(2), 101-121.

Biswal, A. K., Jenamani, M., & Kumar, S. K. (2018). Warehouse efficiency improvement using RFID in a humanitarian supply chain: Implications for Indian food security system. *Transportation Research Part E: Logistics and Transportation Review*, *109*, 205-224.

BnnoBRs, J. (1962). Partitioning procedures for solving mixed-variables programming problems. *Numer. Math*, *4*(1), 238-252.

Chang, Y. S., & Lee, H. J. (2018). Optimal delivery routing with wider drone-delivery areas along a shorter truck-route. *Expert Systems with Applications*, *104*, 307-317.

Chowdhury, P., Paul, S. K., Kaisar, S., & Moktadir, M. A. (2021). COVID-19 pandemic related supply chain studies: A systematic review. *Transportation Research Part E: Logistics and Transportation Review*, *148*, 102271.

D'Andrea, R. (2014). Guest editorial can drones deliver?. *IEEE Transactions on Automation Science and Engineering*, *11*(3), 647-648.

Dorigo, M., & Gambardella, L. M. (1997). Ant colony system: a cooperative learning approach to the traveling salesman problem. *IEEE Transactions on evolutionary computation*, *1*(1), 53-66.

Dorling, K., Heinrichs, J., Messier, G. G., & Magierowski, S. (2016). Vehicle routing problems for drone delivery. *IEEE Transactions on Systems, Man, and Cybernetics: Systems*, *47*(1), 70-85.

Gutjahr, W. J., & Fischer, S. (2018). Equity and deprivation costs in humanitarian logistics. *European Journal of Operational Research*, *270*(1), 185-197.

Gutjahr, W. J., & Nolz, P. C. (2016). Multicriteria optimization in humanitarian aid. *European Journal of Operational Research*, *252*(2), 351-366.

Holguín-Veras, J., Jaller, M., Van Wassenhove, L. N., Pérez, N., & Wachtendorf, T. (2012). On the unique features of post-disaster humanitarian logistics. *Journal of Operations Management*, *30*(7-8), 494-506.

Holguín-Veras, J., Pérez, N., Jaller, M., Van Wassenhove, L. N., & Aros-Vera, F. (2013). On the appropriate objective function for post-disaster humanitarian logistics models. *Journal of Operations Management*, *31*(5), 262-280.

Huang, M., Smilowitz, K., & Balcik, B. (2012). Models for relief routing: Equity, efficiency and efficacy. *Transportation research part E: logistics and transportation review*, *48*(1), 2-18.

Jeong, H. Y., Song, B. D., & Lee, S. (2019). Truck-drone hybrid delivery routing: Payload-energy dependency and No-Fly zones. *International Journal of Production Economics*, *214*, 220-233.

Kilic, A., Dincer, M. C., & Gokce, M. A. (2014). Determining optimal treatment rate after a disaster. *Journal of the Operational Research Society*, *65*, 1053-1067.

McCoy, J. H., & Lee, H. L. (2014). Using fairness models to improve equity in health delivery fleet management. *Production and Operations Management*, *23*(6), 965-977.

Moreno, A., Alem, D., Gendreau, M., & Munari, P. (2020). The heterogeneous multicrew scheduling and routing problem in road restoration. *Transportation Research Part B: Methodological*, *141*, 24-58.

Moshref-Javadi, M., Lee, S., & Winkenbach, M. (2020). Design and evaluation of a multi-trip delivery model with truck and drones. *Transportation Research Part E: Logistics and Transportation Review*, *136*, 101887.

Mourelo Ferrandez, S., Harbison, T., Webwer, T., Sturges, R., & Rich, R. (2016). Optimization of a truck-drone in tandem delivery network using k-means and genetic algorithm. *Journal of Industrial Engineering and Management*, *9*(2), 374-388.

Murray, C. C., & Chu, A. G. (2015). The flying sidekick traveling salesman problem: Optimization of drone-assisted parcel delivery. *Transportation Research Part C: Emerging Technologies*, *54*, 86-109.

Nair, D. J., Grzybowska, H., Fu, Y., & Dixit, V. V. (2018). Scheduling and routing models for food rescue and delivery operations. *Socio-Economic Planning Sciences*, *63*, 18-32.

Najafi, M., Eshghi, K., & Dullaert, W. (2013). A multi-objective robust optimization model for logistics planning in the earthquake response phase. *Transportation research part E: logistics and transportation review*, *49*(1), 217-249.

Pérez-Rodríguez, N., & Holguín-Veras, J. (2016). Inventory-allocation distribution models for postdisaster humanitarian logistics with explicit consideration of deprivation costs. *Transportation Science*, *50*(4), 1261-1285.

Poikonen, S., & Campbell, J. F. (2021). Future directions in drone routing research. *Networks*, *77*(1), 116-126.

Poojari, C. A., & Beasley, J. E. (2009). Improving benders decomposition using a genetic algorithm. *European Journal of Operational Research*, *199*(1), 89-97.

Rodríguez-Espíndola, O., Albores, P., & Brewster, C. (2018). Dynamic formulation for humanitarian response operations incorporating multiple organisations. *International Journal of Production Economics*, *204*, 83-98.

Soleimani, H., Govindan, K., Saghafi, H., & Jafari, H. (2017). Fuzzy multi-objective sustainable and green closed-loop supply chain network design. *Computers & industrial engineering*, *109*, 191-203.

Sun, H., Wang, Y., & Xue, Y. (2021). A bi-objective robust optimization model for disaster response planning under uncertainties. *Computers & Industrial Engineering*, *155*, 107213.

Vu, L., Vu, D. M., Hà, M. H., & Nguyen, V. P. (2022). The two-echelon routing problem with truck and drones. *International Transactions in Operational Research*, *29*(5), 2968-2994.

Wang, X., Wang, X., Liang, L., Yue, X., & Van Wassenhove, L. N. (2017). Estimation of deprivation level functions using a

numerical rating scale. *Production and Operations Management*, *26*(11), 2137-2150.
Wang, Z., & Sheu, J. B. (2019). Vehicle routing problem with drones. *Transportation research part B: methodological*, *122*, 350-364.
Wohlsen, M. (2014). The next big thing you missed: Amazon's delivery drones could work-they just need trucks. https://www.wired.com/2014/06/the-next-big-thing-you-missed-delivery-drones-launched-from-trucks-are-the-future-of-shipping/.
Xiang, Y., & Zhuang, J. (2016). A medical resource allocation model for serving emergency victims with deteriorating health conditions. *Annals of Operations Research*, *236*(1), 177-196.
Yu, L., Zhang, C., Yang, H., & Miao, L. (2018). Novel methods for resource allocation in humanitarian logistics considering human suffering. *Computers & Industrial Engineering*, *119*, 1-20.
Yu, L., Yang, H., Miao, L., & Zhang, C. (2019). Rollout algorithms for resource allocation in humanitarian logistics. *IISE Transactions*, *51*(8), 887-909.
Zhu, L., Gong, Y., Xu, Y., & Gu, J. (2019). Emergency relief routing models for injured victims considering equity and priority. *Annals of Operations Research*, *283*, 1573-1606.